Vol. 23(4), pp.131-141, April 2024
DOI: 10.5897/AJB2024.17662
Article Number: C2C919D72050
ISSN: 1684-5315

http://www.academicjournals.org/AJB

ACADEMIC JOURNALS
expand your knowledge

African Journal of Biotechnology

Full Length Research Paper

In vitro antifungal potential of citral and nanoencapsulated citral against *Fusarium oxysporum* f.sp. *lycopersici*

Portia Osei-Obeng[1]*, Leonard Muriithi Kiirika[2] and Aggrey Bernard Nyende[2]

[1]Department of Molecular Biology and Biotechnology, Pan African University, Institute for Basic Sciences, Technology and Innovation, Nairobi, P. O. Box 62000-00200, Kenya.
[2]Department of Horticulture and Food Security, Jomo Kenyatta University of Agriculture and Technology, Nairobi, P. O. Box 62000-00200, Kenya.

Received 6 March 2024; Accepted 4 April 2024

This study aimed to encapsulate citral in chitosan nanoparticles and test its antifungal activity, along with the nanoparticles, against *Fusarium oxysporum f.sp. lycopersici* (FOL), a soil-borne pathogen causing worldwide yield losses in tomato production. The nanoparticles were characterized using scanning electron microscopy (SEM), FT-IR, encapsulation efficiency (EE), loading capacity (LC), and in vitro release pattern. SEM images revealed a spherical morphology with particle sizes ranging from 33 to 301 nm. EE and LC ranged from 2.9 to 7.2% and from 0.6 to 1.3%, respectively. The in vitro release exhibited a controlled pattern. Citral completely inhibited FOL mycelial growth at 500 µg/mL, with MIC/MFC determined at 512 µg/mL, whereas the nanoparticles achieved maximum mycelial inhibition (27%) at 1000 µg/mL, with MIC at 4096 µg/mL. Our study reveals citral as a potent biofungicide against FOL; however, further research is required to assess its in vivo activity. Increasing concentrations of the nanoparticles and the addition of copolymers to the chitosan-tripolyphosphate system for encapsulation of citral may enhance its potential for use as an antifungal agent.

Key words: Chitosan, nanoencapsulation, citral, antifungal, *Fusarium oxysporum* f.sp. *lycopersici.*

INTRODUCTION

Fusarium oxysporum f.sp. lycopersici (FOL), a soil-borne fungus, is the phytopathogen responsible for causing fusarium wilt in tomatoes. This devastating disease leads to significant global losses in tomato yields in the field, greenhouses, and high tunnels (Devi et al., 2022). The pathogen can persist in the soil for extended periods, even without a host (Sharma et al., 2017). FOL primarily infects the roots of tomato plants and subsequently colonizes the vascular tissues, disrupting the function of xylem vessels and leading to wilting, stunted growth, and plant death (Kalleli et al., 2020).

Current management of the pathogen mainly relies on chemical fungicides such as carbendazim and prochloraz (Srinivas et al., 2019). However, due to the adverse environmental and health effects, there is a pressing need to explore and adopt alternative, sustainable, and

*Corresponding author. E-mail: obengoseiportia@gmail.com.

eco-friendly control methods that can be used either independently or integrated into management systems for *Fusarium* wilt in tomatoes (Sharma et al., 2017).

A wide array of organic compounds known as secondary metabolites are produced by plants, playing an essential role in their defense against biotic and abiotic stresses (Yang et al., 2018). Among these secondary metabolites, essential oils (EOs) have garnered significant attention and have been extensively researched for their antifungal activity against disease-causing fungi (Lammari et al., 2020). Essential oils (EOs) containing cinnamaldehyde, citral, eugenol, thymol, and carvacrol as active compounds have been identified as particularly effective in combating these microbes (Bassolé and Juliani, 2012). Citral, a major active compound found in lemongrass and *Litsea cubeba* essential oils, has been investigated for its antifungal potential against various phytopathogenic fungi, including some members of the *F. oxysporum* species (Kaur et al., 2019). Citral's antifungal activity has been attributed to its ability to penetrate the cell membrane, altering membrane permeability and leading to cell leakage and fungal death (Kaur et al., 2019).

However, citral's susceptibility to oxidation, poor solubility in water, high volatility, and poor stability when exposed to open conditions limit its use in its pure form, similar to most essential oils (Ma et al., 2020). Therefore, to fully harness the antifungal potential of citral in plant protection, its formulation in a suitable carrier for efficient delivery is imperative. Agricultural research has gradually shifted from conventional to novel technologies like nanotechnology to aid in plant protection and overall crop production. Nanotechnology is being investigated for various purposes, including plant hormone delivery, controlled release of agrochemicals, and bioremediation (Worrall et al., 2018). Nanoparticles can serve as plant protectants themselves or as carriers for agrochemicals and active compounds (Worrall et al., 2018). As carriers, they enhance shelf-life, improve water solubility, reduce toxicity, promote site-specific uptake to the target pathogen, and increase the efficacy, stability, and bioavailability of the active compounds (Worrall et al., 2018).

A wide range of nanomaterials exists for use as nanoparticle carriers, including organic (polymers, proteins, carbohydrates), inorganic (metals, metal oxides), or carbon-based materials (Oleandro et al., 2024). Zein, a hydrophobic plant protein-based nanomaterial, has been explored as a nanocarrier for plant protection (Liu et al., 2023). Zein nanoparticles have been utilized to encapsulate *Zataria multiflora* and tested against wheat-pathogenic fungi and bacteria (Rasteh et al., 2024). Nunes et al. (2024) also encapsulated orange essential oil in zein nanoparticles and investigated its efficacy against *Fusarium* incidence during agroecological maize seed storage, showing that the zein-encapsulated oil performed significantly better than the pure oil. Alginate, an organic nanomaterial, is a hydrophilic biopolymer derived from brown algae and some bacteria. Alginate alone as a polysaccharide has been explored in the control of *Alternaria solani and F. oxysporum f.sp. albedinis* in tomato and date palm, respectively (Dey et al., 2019; Bouissil et al., 2022). Santos et al. (2023) co-encapsulated tea tree oil and *Cucumis sativa* seed oil in an alginate matrix and evaluated the system's ability to inhibit microorganisms and prolong fruit shelf-life.

Chitosan, a biopolymeric nanomaterial derived from the deacetylation of chitin, has been extensively explored due to its non-toxicity, biodegradability, bioavailability, biocompatibility, safety, and inherent antimicrobial properties (Xing et al., 2015). The antimicrobial properties of chitosan have been demonstrated in plants such as tomatoes, kiwifruit, and apples (Abdel-Rahman et al., 2021; Beatrice et al., 2017; Kiirika et al., 2013). Mechanisms of action of chitosan's antimicrobial activity include the interaction of the positive amino groups with negatively charged microbial surfaces, leading to membrane damage and alteration of membrane permeability, as well as deposition onto the microbial surface, which prevents the entry of nutrients and the outflow of metabolites for excretion (Xing et al., 2015). Chitosan has been widely used in the encapsulation of essential oils (EOs) and active compounds such as clove essential oil, eugenol, thymol, nettle essential oil, *Nepta hormozganica, and Nepta dschuprensis* essential oils (Hadidi et al., 2020; Oluoch et al., 2021; Bagheri et al., 2021; Amighi et al., 2023). The small size, high surface area, and target-specific properties of nanoparticles make them more advantageous in plant protection as they allow penetration of pathogen membranes (Hoang et al., 2022).

Although citral has been encapsulated in solid-lipid nanoparticles, nano-lipid carriers, chitosan/carboxymethyl cellulose copolymer to form hydrogel microspheres, and nano-emulsion, to the best of our knowledge, there is little or no information on the encapsulation of citral in pure chitosan nanoparticles via ionic gelation and its utilization as an antifungal agent for plant protection. Furthermore, while the antifungal activity of citral has been tested against plant pathogens and even members of the *F. oxysporum* species complex, there is a lack of data regarding its specific effect on *F. oxysporum f.sp. lycopersici*. Therefore, this study aimed to synthesize and characterize citral-loaded chitosan nanoparticles and assess the antifungal activity of the nanoparticles and pure citral against *F. oxysporum f.sp. lycopersici.*

MATERIALS AND METHODS

Chemical reagents

Citral (purity: 95%), chitosan (low molecular weight, degree of deacetylation ≥90%), and resazurin sodium salt were purchased from Glentham Life Sciences (Corsham, UK). Sodium tripolyphosphate (TPP) was obtained from Sigma-Aldrich (Missouri, USA). Potato dextrose agar and broth were sourced from Scharlab

(Barcelona, Spain), and carbendazim was acquired from Solarbio Life Science (Beijing, China). Tween 20 and 80, ethanol (purity: 95%), glacial acetic acid, and hydrochloric acid (concentration: 35%) were obtained from Legacy Lab Africa (Nairobi, Kenya).

Fungal strain

The *F. oxysporum f.sp lycopersici* pathogen was obtained from the Kenya Plant Health Inspectorate Services (KEPHIS, Kenya). The pathogen was maintained on Potato Dextrose Agar (PDA) supplemented with 30 mg/mL streptomycin sulfate to inhibit bacterial growth. Slants of the pathogen were also prepared on half-strength PDA with glycerol for long-term storage purposes.

Synthesis of citral-loaded chitosan nanoparticles

Citral-loaded chitosan nanoparticles were synthesized using the ionic gelation method, following the procedure described by Hosseini et al. (2013) with slight modifications. To prepare a chitosan solution (1.5% w/v), chitosan was dissolved by shaking in aqueous acetic acid (1% v/v) at 25°C overnight for 24 h. In a 40 mL volume of chitosan solution, Tween 80 was added as a surfactant and stirred at 45°C for 2 h to obtain a homogeneous mixture. Citral at varying weights (0, 0.15, 0.30, 0.45, and 0.60 g) was gradually added to the above mixture and agitated for 20 min, resulting in chitosan-to-citral weight ratios of 1:0, 1:0.25, 1:0.50, 1:0.75, and 1:1.00, respectively. TPP (0.5% w/v) was then added drop-wise to the emulsion under continuous stirring, and agitation was carried out for 40 min. The formed nanoparticles were separated by centrifugation of the solution at 4000 rpm for 30 min at 25°C. The collected wet particles were washed three times with distilled water under the same centrifugation conditions. To ensure the formation of a homogeneous suspension, the cleaned wet particles were dispersed in 25 mL of distilled water using a probe sonicator in an ice bath for 4 min with a 2 s sonication and 1 s rest sequence. The resulting homogeneous suspensions were then freeze-dried at -65°C for 72 h. The freeze-dried nanoparticles were subsequently stored at 4°C until further use and analysis.

Characterization of nanoparticles

Determination of particle size and morphology

The size and morphology of the prepared nanoparticles were analyzed using a scanning electron microscope (FEI Helios NanoLab 600, Hillsboro, OR, NIST-USA), following the method described by Hosseini et al. (2013). Fourier-transform infrared spectroscopy (FTIR) analysis was conducted using an IRAffinity-1S FTIR spectrophotometer (Shimadzu Corp., 031891) equipped with an ATR to determine the functional groups on the surface of chitosan nanoparticles, citral, and the citral-loaded chitosan nanoparticles. The sample holder was filled with 1 mg of the sample, and the instrument was set up to perform a total of 20 scans with a 4 cm^{-1} spectral resolution for both background and sample spectra, recorded rapidly in the range between 4000 to 400 cm^{-1}.

Determination of encapsulation efficiency (EE %) and loading capacity (LC %)

The amount of citral encapsulated in chitosan nanoparticles was determined by UV-vis spectrophotometry following the method described by Hosseini et al. (2013). To achieve this, 10 mg of citral-loaded chitosan nanoparticles were mixed in 4 mL of 2M HCl and boiled at 95°C for 30 min. After cooling, 2 mL of ethanol was added to the homogeneous mixture and centrifuged at 9000 rpm for 5 min at 25°C. The supernatant was analyzed for citral content using UV-vis spectrophotometry at 298.5 nm. The amount of citral was calculated using the calibration curve of free citral (0.02, 0.04, 0.06, 0.08, and 0.10%) in absolute ethanol. Chitosan nanoparticles underwent a similar process as citral-loaded chitosan nanoparticles and were used as blanks. Each sample was recorded in triplicate. Loading capacity and encapsulation efficiency were estimated from Equations (1) and (2).

$$EE\% = \frac{\text{weight of loaded compound}}{\text{weight of initial compound}} \times 100 \quad (1)$$

$$LC\% = \frac{\text{weight of the loaded compound}}{\text{weight of NPs after freeze drying}} \times 100 \quad (2)$$

In vitro release study

The in vitro release study of citral from chitosan nanoparticles was conducted in different media (PBS and acetate buffer) at different pH (7.4 and 5), respectively, using the dialysis method as described by Shetta et al. (2019). Briefly, 40 mg of freeze-dried citral-loaded chitosan nanoparticles (1:0.50 w/w) was placed in a dialysis bag (12,000-14,000 kDa) containing 2 mL of the release media (PBS or acetate buffer) and placed in a 50 mL tube containing 13 mL of the same release media, incubated at room temperature under gentle shaking. At every time interval of 12 h, 5 mL of release media in the 50 mL tube was taken for analysis and an equal volume of fresh release media was added. The total cumulative amount of citral (mg) in the release medium (mL) volume encapsulated in the nanoparticles was quantified spectrophotometrically. The release was quantified as described by Oluoch et al. (2021):

$$\text{Release } \% = \frac{\text{Released oil}}{\text{Total oil}} \times 100 \quad (3)$$

Antifungal activity evaluation

Mycelial growth inhibition

The antifungal activity of pure citral and the citral-loaded chitosan nanoparticles (1:0.50 w/w chitosan to citral weight ratio) was assessed using the poisoned food technique described by La Torre et al. (2016). Citral and the nanoparticles were dissolved in 0.5% Tween 20 made with sterile distilled water. Potato dextrose agar (PDA) was prepared in distilled water and autoclaved at 121°C for 15 min, allowed to cool, and maintained at a molten state (45°C) in a water bath (45±1°C). The products (citral and nanoparticles) were then added to 20 mL of molten PDA and poured into 90 mm Petri dishes to achieve final concentrations of 250, 500, 750, and 1000 µg/mL. Carbendazim at 100 µg/mL dissolved in 0.5% Tween 20 was used as the positive control, and 0.5% Tween 20 was used as the negative control. After allowing the agar to solidify, the plates were inoculated at the center with 5 mm diameter mycelial plugs cut from the peripheral areas of a 7-day-old pre-cultured FOL. The plates were sealed with parafilm and incubated at 25±1°C until the growth in the control reached the edges of the plates. Percentage mycelial inhibition was calculated relative to the control using the

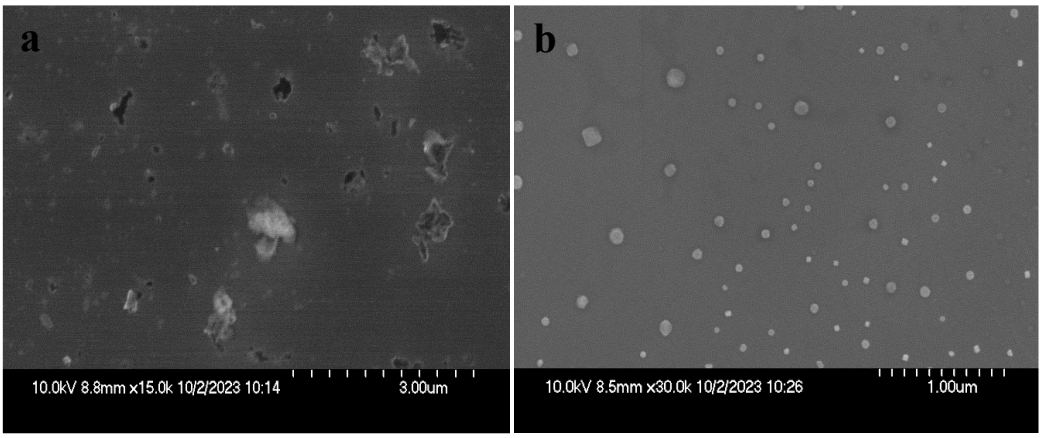

Figure 1. SEM micrograph of (a) chitosan nanoparticles and (b) citral-loaded chitosan nanoparticles made with chitosan to citral ratio of 1:0.50 (w/w).

formula proposed by Chun and Chandrasekaran (2019):

$$Percent\ Inhibition = \frac{(Mc - Mt)}{Mc} \times 100 \quad (4)$$

Where Mc is the mycelial growth in control and Mt is the mycelial growth in treatment.

Determination of minimum inhibitory and fungicidal concentrations

The broth micro-dilution method was employed to determine the minimum inhibitory concentrations (MICs) of citral and nanoparticles, as described by Sharma et al. (2017). The inoculum suspension was prepared by culturing *F.oxysporum f.sp. lycopersici* (FOL) at 25±1°C on Potato Dextrose Agar (PDA) for 7 days. The dishes were flooded with 10-15 mL sterile distilled water, and spores were carefully scraped off. The suspension was filtered through sterile cheesecloth to remove mycelial fragments, vortexed for 15 s to ensure homogeneity, and quantified using a hemocytometer. A final inoculum concentration of 2-2.5 × 10^5 cells/mL was used for the assay. Resazurin was prepared by dissolving 270 mg of the powder in 40 mL of sterile distilled water. A two-fold serial dilution ranging from 4096 to 8 µg/mL was prepared for both citral and nanoparticles. Each 100 µL of the dilutions received 20 µL of the inoculum suspension and 30 µL of resazurin. Positive control wells contained broth, inoculum suspension, and resazurin, whereas negative control wells contained only broth and resazurin to check the sterility of the broth. The plates were then incubated at 28±1°C for 48 h. The experiments were performed in triplicate, and the minimum inhibitory concentration was determined as the lowest concentration at which there was no color change. To determine the minimum fungicidal concentration (MFC), 10 µL of the wells with no color change were plated on PDA plates supplemented with 30 mg/mL streptomycin sulfate. The plates were incubated at 28±1°C for 72 h, and the lowest concentration at which no visible fungal growth was observed was taken as the MFC.

Statistical analysis

The average particle size was determined from SEM images using ImageJ 1.54d (http://imagej.org) and analyzed using Microsoft Excel 2013. Data on the effects of the treatments on the mycelial growth of *F. oxysporum f.sp. lycopersici* were analyzed using a one-way analysis of variance and means comparison using Tukey's test at a significance level of $p < 0.05$. The statistical analyses used R v.4.3.1 and Origin 2023 learning edition.

RESULTS AND DISCUSSION

Particle size and morphology distribution

The SEM images of the chitosan nanoparticles and the citral-loaded chitosan nanoparticles revealed irregular particle shapes and distributions, as depicted in Figures 1a and b. This irregularity in shape and distribution can be attributed to the potential instability encountered during the preparation process, as previously reported by Hosseini et al. (2013), and is consistent with the findings of Haider et al. (2017). Interestingly, the citral-loaded chitosan nanoparticles exhibited a distinctive spherical shape, while the unloaded chitosan nanoparticles appeared somewhat collapsed. This discrepancy in shape may be attributed to the reduced turgidity of the unloaded nanoparticles, resulting in instability of surface morphology, as suggested by Kalagatur et al. (2018). It's noteworthy that our observations deviated from some previous studies where chitosan nanoparticles encapsulating essential oil active compounds such as eugenol, thymol, and carvacrol displayed regular nanoparticle distributions and spherical shape for the unloaded chitosan nanoparticles, as reported by Keawchaoon and Yoksan (2011) and Oluoch et al. (2021).

The average size of the unloaded chitosan nanoparticles, as outlined in Table 1, was 99 nm. In contrast, the size of the citral-loaded chitosan nanoparticles exhibited a range from 33 to 301 nm, which notably falls within the acceptable size range (10 to 1000

Table 1. Average particle size of chitosan nanoparticles and citral-loaded chitosan nanoparticles and encapsulation efficiency (EE%) and loading capacity (LC%) of citral in citral-loaded chitosan nanoparticles by UV-Vis spectrophotometry.

Chitosan:citral ratio (w/w)	Average particle size (nm)[a]	EE (%)[b]	LC (%)[c]
1:0	99.00±34.00	0.00	0.00
1:0.25	94.00±29.00	5.20	0.60
1:0.50	301.00±130.00	7.20	0.90
1:0.75	72.80±26.83	4.00	1.03
1:1.00	33.32±5.93	2.90	1.31

[a] Results were reported as mean ± SD. [b,c] Results are means of triplicate data, and the standard deviation is 0.00.

nm) for nanoparticles fabricated with biopolymers like chitosan, as corroborated by Khanmohammadi et al. (2015). Unlike in previous studies where particle size increased as a function of increased oil content (Hosseini et al., 2013; Shetta et al., 2019), in this study, after the citral content of 0.50%, particle size began to decrease. This phenomenon may have been due to the interactions of the citral and the chitosan leading to more compact and smaller nanoparticles with an increase in initial citral content (Begines et al., 2020; Jia et al., 2020). However, particle size decreased with increased extract content in studies where plant extracts from Arrabidaea chia and Mentha longifolia were encapsulated in chitosan nanoparticles (El-Aziz et al., 2018; Servat-Medina et al., 2015). Additionally, a study on the encapsulation of krill oil in chitosan nanoparticles observed a similar phenomenon (Haider et al., 2017).

Fourier Transform Infrared Spectroscopy (FTIR) characterization

FTIR spectra of chitosan nanoparticles, citral, and citral-loaded chitosan nanoparticles (1:0.50 chitosan to citral ratio) are shown in Figure 2. Chitosan nanoparticles exhibited a characteristic broad peak at 3418 cm^{-1}, attributed to the presence of O-H and N-H stretching groups, a peak at 1535 cm^{-1} (amide II), and a peak at 1220 cm^{-1} (C-O-C stretch). These peaks indicate how the NH_3+ groups of chitosan and the phosphoric groups of the tripolyphosphate used as the cross-linker interact electrostatically to form the chitosan nanoparticles spontaneously (Hosseini et al., 2013).

Pure citral (95%) exhibited characteristic peaks at 2922 cm and 2856 cm^{-1}, which can be assigned to C-H stretching vibration, a strong absorption band at 1674 cm^{-1} (C=O stretching vibration), 1445 cm^{-1} (C=C vibration), and 1380 cm^{-1} (CH3 bending) (Zhu et al., 2015). The citral-loaded chitosan nanoparticles showed peaks that could be found in both the chitosan nanoparticles and pure citral (Figure 2c). The 2929 cm^{-1} (C-H stretching) peak present in the citral-loaded chitosan nanoparticles but absent in the chitosan nanoparticles indicates the increased ester groups, which may be from the citral, suggesting the successful encapsulation of citral into the chitosan nanoparticles (Keawchaoon and Yoksan, 2011). The shift of the peak at 1674 cm^{-1} in pure citral to 1734 cm^{-1} in the citral-loaded chitosan nanoparticles also indicates the presence of an ester group, which may have originated from the citral, further indicating the successful encapsulation of citral into the chitosan nanoparticles (Tian et al., 2018).

Encapsulation efficiency and loading capacity

Encapsulation efficiency (EE%) and loading capacity (LC%) of citral in the citral-loaded chitosan nanoparticles were determined using UV-Vis spectrophotometry. The maximum absorbance of citral was found at 298.5 nm, and a calibration curve (R^2 = 0.9749) was constructed for citral (0.02, 0.04, 0.06, 0.08, and 0.10%) in absolute ethanol. The percentages of EE and LC were calculated using Equations (1) and (2), respectively, as shown in Table 1. The EE% of citral ranged from 2.9 to 7.2%, with the maximum EE% achieved at 1:0.50 (w/w) chitosan to citral ratio. EE% decreased with increasing initial citral content, which may be attributed to the saturation point reached when loading citral into the chitosan nanoparticles, consistent with earlier findings (Haider et al., 2017; Hosseini et al., 2013; Shetta et al., 2019).

The relatively low encapsulation of citral might result from the hydrophobic nature of citral, posing challenges in achieving uniform dispersion within the chitosan solution and citral's instability in acidic environments (Maswal and Dar, 2014). Nevertheless, further optimization of the chitosan-tripolyphosphate encapsulation system parameters, the addition of copolymers, and the use of different nanocarrier system forms may enhance the encapsulation efficiency of citral (Jia et al., 2020; Khanmohammadi et al., 2015; Worrall et al., 2018). Conversely, LC% of citral ranged from 0.6-1.3%. Unlike EE%, LC% increased with the rise in initial citral content, consistent with observations made in

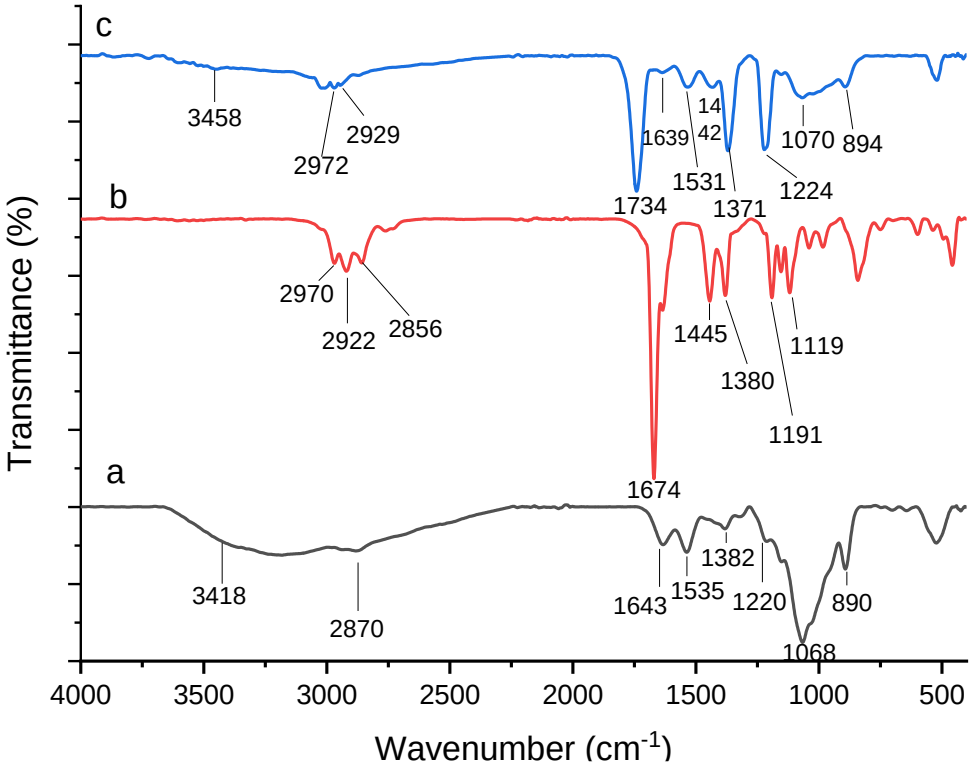

Figure 2. FTIR spectra of (a) chitosan nanoparticles, (b) citral and (c) citral-loaded chitosan nanoparticles with chitosan to citral weight ratio of 1:0.50 (w/w).

previous studies related to loading carvacrol and oregano essential oil into chitosan-TPP systems (Hosseini et al., 2013; Keawchaoon and Yoksan, 2011). The 1:0.50 (w/w) chitosan to citral ratio was chosen as the optimal formulation for the rest of the study.

In vitro release of citral from chitosan nanoparticles

The *in vitro* release investigation of citral from the citral-loaded chitosan nanoparticles (1:0.50 (w/w) chitosan to citral ratio) (Figure 3) was conducted in different pH media: PBS (pH 7.4) and acetate buffer (pH 5) for 72 h to confirm the successful encapsulation of citral in the chitosan nanoparticles and determine the ideal pH condition for the release of citral from the nanoparticles (Keawchaoon and Yoksan, 2011). Generally, diffusion, surface erosion, disintegration, and desorption are the various mechanisms by which a drug or oil is released from micro and nanoparticles (Hosseini et al., 2013). The release pattern of citral from chitosan nanoparticles can be described as a biphasic process with two distinct phases: an initial burst release followed by a subsequent sustained slower release, which aligns with previous findings related to the release of oregano, thymol, and eugenol from chitosan nanoparticles (Hosseini et al., 2013; Oluoch et al., 2021).

In the first 12 h, an initial burst release occurred, with citral being released up to 39.2 and 43.5% in PBS (pH 7.4) and acetate buffer (pH 5), respectively. This initial burst release may be attributed to the citral molecules attached to the surface of the nanoparticles and those encapsulated in proximity to the surface. As the dissolution rate of the polymer is elevated near the surface, there is also a substantial release of the drug, citral, in this study (Anitha et al., 2011). The release of citral in the second phase showed a slow release pattern, with citral being released up to 62.1 and 75.2% in PBS (pH 7.4) and acetate buffer (pH 5), respectively, at the end of the 72-h period. This slow release in the second phase could be attributed to the diffusion of citral from the chitosan nanoparticles (Oluoch et al., 2021). The release occurred more rapidly under acidic conditions compared to neutral conditions. In an acidic environment, the protonation of the amino groups on the surface of the chitosan nanoparticles causes the polymer matrix to swell, facilitating the quicker release of the drug (Anitha et al., 2011). These findings align with previous studies, where the release of carvacrol from the chitosan-TPP nanoparticles system and curcumin from dextran sulfate-chitosan nanoparticles in pH 3 and pH 5 showed a more rapid release than in neutral conditions (Anitha et al., 2011; Keawchaoon and Yoksan, 2011).

It is worth noting that the release of citral was not

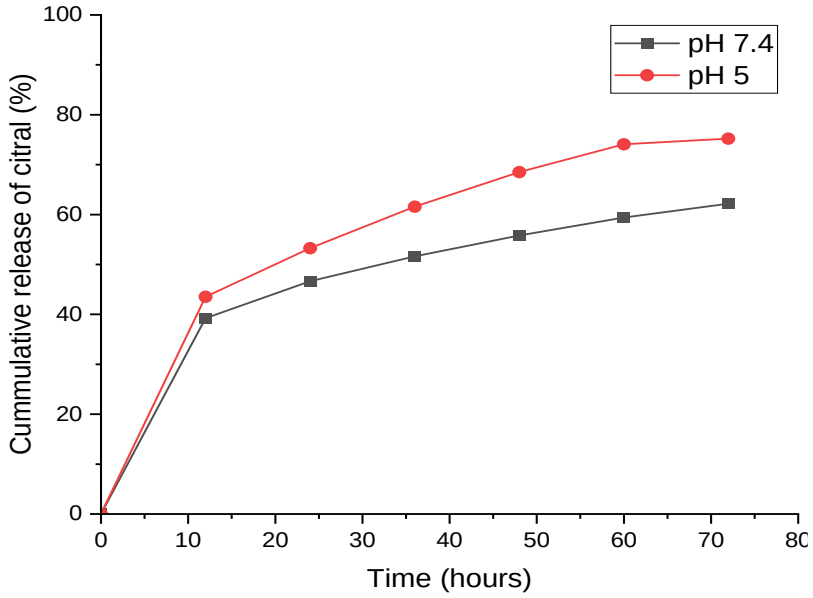

Figure 3. *In vitro* release profile of citral from chitosan nanoparticles in different pH media.

complete, as a complete release would require the total degradation of the chitosan nanoparticles (Shetta et al., 2019). Optimum tomato performance is achieved in a well-drained, light loam soil with a pH of 5 to 7, indicating that more than 70% of citral oil will be released in an ideal pH of 5 if used in field studies.

Mycelia growth inhibition

The results of the mycelial growth and inhibition assay of *F. oxysporum f.sp lycopersici* (FOL) by citral and citral-loaded chitosan nanoparticles are presented in Figure 4, and their values are reported in Table 2. Both citral and its nanoparticles exhibited inhibitory effects on FOL mycelial growth, albeit in a dose-dependent manner. The negative control (0.5% Tween 20) showed a mean growth of 85.7±0.67 mm (Figure 4C(j)), whereas the positive control (100 µg/mL carbendazim) completely inhibited the mycelial growth of the test fungus (Figure 4C (i)). Carbendazim, a broad-spectrum systemic fungicide, has been used to control fusarium wilt of tomatoes and other plant-pathogenic fungi (Ayesha et al., 2021). Yassin et al. (2021) revealed that carbendazim, at a low concentration of 0.50 ppm, could completely inhibit the mycelial growth of *F. proliferatum*. These previous findings demonstrate the effectiveness of carbendazim in managing fungal diseases; nevertheless, the World Health Organization classifies carbendazim as a hazardous chemical, hence the need to find more environmentally friendly ways of crop protection (Li et al., 2020).

Citral at a concentration of 250 µg/mL (Figure 4A(a)) showed mycelial inhibition of 40.5%. With increased concentrations (500, 750, and 1000 µg/mL) (Figure 4A(b, c, d)), it completely inhibited the growth of FOL, showing 100% mycelial inhibition (Table 2). This dose-dependent inhibition aligns with previous findings where citral was tested against plant fungal pathogens (Wei et al., 2021). Citral at a concentration of 20 µL/L inhibited the growth of *F. oxysporum* (Linde et al., 2010) completely. The study also demonstrated citral as being more active than the two essential oils used, suggesting citral as the main compound influencing the antifungal activity of the essential oils. Previous studies have shown that citral's antifungal potential may be due to its ability to cross the plasma membrane of phytopathogenic fungi and interact with the membrane's proteins and enzymes. Monoterpene-membrane protein interactions alter hyphae and plasma membrane morphology, causing fungal cell death (Kaur et al., 2019).

The maximum inhibition by the nanoparticles was recorded at 27.16% at a concentration of 1000 µg/mL. A comparison of the mycelial inhibition of pure citral and its nanoparticles showed a significant difference in mycelial inhibition, where citral proved more active and potent than its nano-encapsulated counterpart. This finding contrasts with previous research where nano-emulsions of citral exhibited higher antibacterial activity than pure citral (Marei et al., 2018). Sharma et al. (2023) encapsulated citral in chitosan nanoparticles prepared using chitosan sulfate, a derivative of chitosan, and their results showed that nano-encapsulated citral performed better than pure citral in quorum sensing inhibition. Kalagatur et al. (2018) reported improved antifungal activity of nano-encapsulated *Cymbopogon martinii*

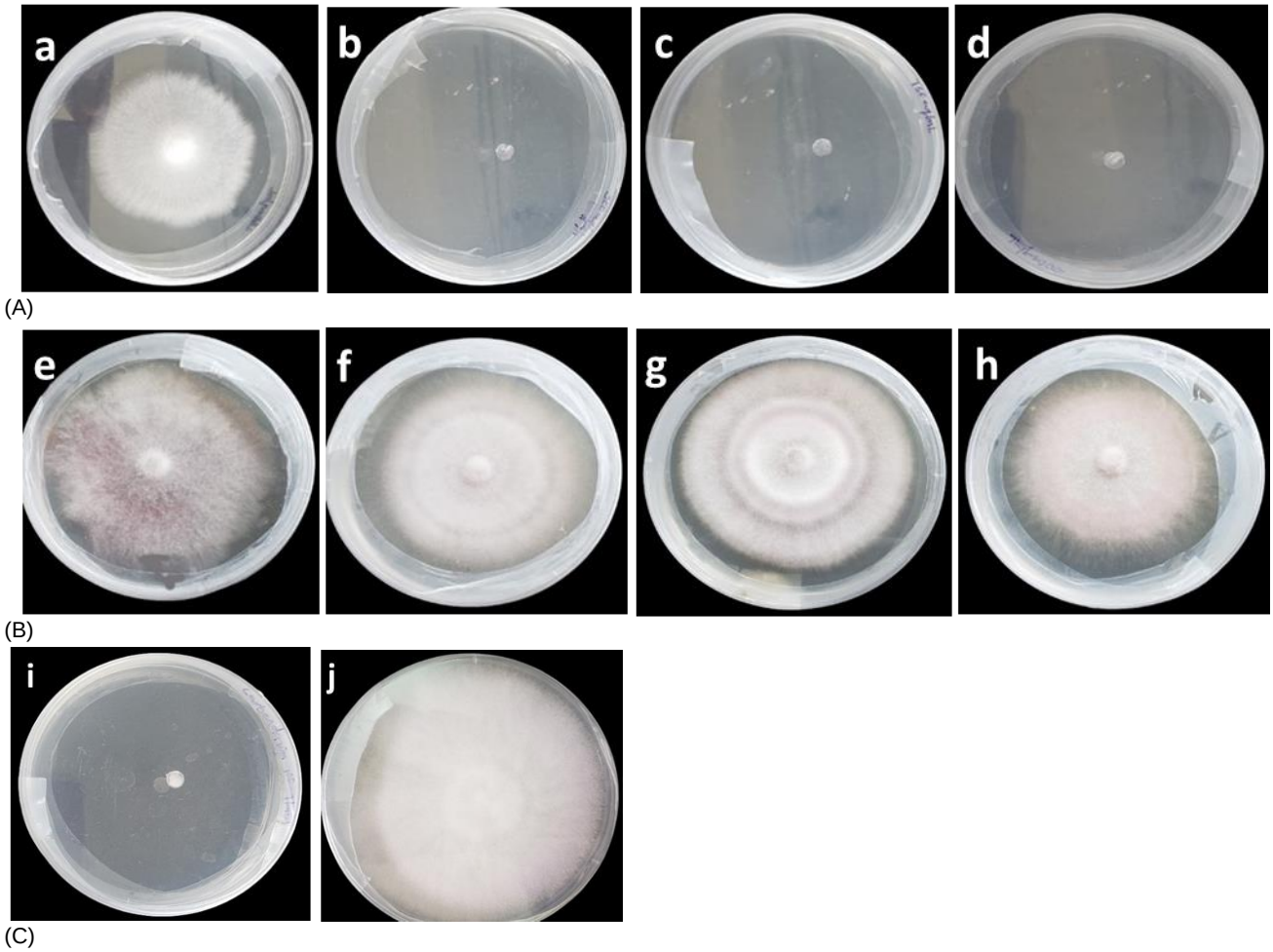

Figure 4. Mycelial growth inhibition of FOL plates treated with (A) citral: (a) 250µg/mL, (b) 500µg/mL, (c) 750µg/mL, and (d) 1000µg/mL; (B) citral-loaded chitosan nanoparticles (1:0.50 chitosan to citral weight ratio): (e) 250µg/mL, (f) 500µg/mL, (g) 750µg/mL and, (h) 1000µg/mL; (C) control: (i) 100µg/mL carbendazim and, (j) 0.5% Tween 20.

essential oil against *F. graminearum*. Cai et al. (2023) loaded *Athyrium sinense* essential oil against *Pectobacterium carotovorum sp. Carotovorum*, and the nanoparticles exhibited significant antibacterial activity against the pathogen. Thymol encapsulated in chitosan nanoparticles and tested against *Botrytis cinerea* by Zhao et al. (2023) also showed higher antifungal activity than unencapsulated thymol.

The significantly lower mycelial inhibition by the citral-loaded chitosan nanoparticles may be attributed to its low encapsulation efficiency (7.2%), as seen in Table 1, and perhaps a situation of incompatibility between the chitosan nanocarrier and citral oil, particularly during the ionic gelation process to form the nanoparticles. This antifungal activity may be improved if the concentration of the citral-loaded chitosan nanoparticles is increased, as demonstrated in Table 2, where an increase in nanoparticle concentration from 250 to 1000 µg/mL significantly increased mycelial growth inhibition. However, cost considerations may arise with increasing concentrations to boost antifungal activity.

Nonetheless, employing different encapsulation methods like coacervation, spray-drying, nanoprecipitation, or a combination of these methods could enhance the encapsulation efficiency of citral oil and subsequently increase its antifungal activity, as shown in previous studies (Lü et al., 2018; Jian et al., 2019). Furthermore, optimization of encapsulation parameters like pH, temperature, stirring speed, and time, the addition of copolymers like alginate, and the use of co-surfactants in the chitosan-tripolyphosphate encapsulation system could also help in improving the encapsulation efficiency of citral oil in the chitosan nanoparticles and ultimately its antifungal activity (Nagpal et al., 2010). Additionally, different carrier materials like zein and maltodextrin could be utilized for the encapsulation of citral oil to ensure the uniform dispersion of citral and enhance its encapsulation (Yammine et al.,

Table 2. Mycelia growth inhibition of different concentrations of citral and its nanoparticles against *Fusarium oxysporum* f.sp. *lycopersici*.

Treatment	Concentration (µg/mL)	Mycelial Growth (mm)	MGI%
Citral	250	51.00±0.58^{d}	40.50
	500	00.00±0.00^{e}	100.00
	750	00.00±0.00^{e}	100.00
	1000	00.00±0.00^{e}	100.00
CCNPs	250	75.70±1.20^{b}	11.68
	500	68.70±2.03^{bc}	19.80
	750	65.70±1.76^{c}	23.33
	1000	62.30±3.71^{c}	27.16
Carbendazim	100	00.00±0.00^{e}	100.00
Negative control	0.5% Tween 20	85.70±0.67^{a}	-

Values within columns followed by same letter are not significantly different by Tukey's test ($p < 0.05$). Results are means of 3replicates ±Standard Error (SE), MGI %: percent mycelial growth inhibition, CCNPs: citral-loaded chitosan nanoparticles (1:0.50 chitosan to citral weight ratio).

Table 3. Minimum inhibitory concentration (MIC) and minimum fungicidal concentration (MFC) of citral and its nanoparticles against *Fusarium oxysporum* f.sp *lycopersici.*

Treatment	MIC (µg/mL)	MFC (µg/mL)
Citral	512	512
Citral-loaded chitosan nanoparticles	4096	ND

Not determined- indicates no MIC or MFC. Values are means of triplicate data and, standard deviation is 0.00.

2023).

Minimum inhibitory and fungicidal concentrations (MIC & MFC)

Citral exhibited strong antifungal effectiveness with MIC and MFC values measured at 512 µg/mL. The identical MIC and MFC values for citral suggest a fungicidal effect occurring at the same concentration that initially inhibits growth, indicating that citral may act as a compound fungicide against FOL (Scorzoni et al., 2016). Previous findings, however, regarding the antifungal activity of citral against other plant fungal pathogens, depict citral as fungistatic since the MIC and MFC values are different. This difference in results could stem from fungal species variability, varying concentrations used, as well as differences in unit measurements and methodologies.

The MIC of citral-loaded chitosan nanoparticles was determined at 4096 µg/mL, while its MFC was not determined due to the range of concentrations used, as shown in Table 3. This result is consistent with the findings in the antifungal activity assay section (3.5) for mycelial growth inhibition, where citral proved more potent at lower concentrations compared to nano-encapsulated citral. The reasons for this discrepancy may be similar to those discussed previously in that section.

CONCLUSIONS AND FUTURE WORKS

This study successfully encapsulated citral within chitosan nanoparticles, as confirmed by SEM and FTIR analysis. The *in vitro* release profile also demonstrated an initial burst release followed by a slower release of citral from the nanoparticles. However, concerning antifungal activity, the mycelial growth inhibition assay revealed that pure citral exhibited significantly higher effectiveness against the pathogen than nano-encapsulated citral, even though the nanoparticles also inhibited the mycelial growth of the pathogen. The MIC and MFC values for pure citral were determined at a concentration of 512 µg/mL, suggesting that citral may serve as a potent antifungal agent against FOL. However, the MIC of the nanoparticles was

observed to be high at 4096 µg/mL, and its MFC was not determined.

Considering the findings from this study, citral in its pure form proved to be a potent antifungal agent against FOL and hence can be considered during the development of alternative fungicides against FOL. Nevertheless, further in vivo studies are essential to confirm its efficacy against this soil-borne pathogen. On the other hand, our findings indicate that the encapsulation of citral did not significantly improve its inhibitory activity. This suggests that an increase in the concentration of the nano-encapsulated citral, optimization of the encapsulation process of citral into the chitosan-tripolyphosphate system, and the addition of copolymers may improve its efficacy. Additionally, the use of different nanocarrier systems and encapsulation methods or a combination of these methods could also increase its encapsulation efficiency and subsequent antifungal activity.

CONFLICT OF INTERESTS

The authors have not declared any conflict of interests.

ACKNOWLEDGMENTS

The authors would like to express their gratitude to the African Union Commission for their generous scholarship and research funding that enabled this study. They also extend their thanks to the Institute for Biotechnology Research (IBR) at Jomo Kenyatta University of Agriculture and Technology (JKUAT) for granting access to their molecular biology lab for laboratory work. Additionally, the authors appreciate the valuable contributions made by Ifeoluwa Deborah Gbala (Trieste, Italy) to this research.

REFERENCES

Abdel-Rahman FA, Monir GA, Hassan MSS, Ahmed Y, Refaat MH, Ismail IA, El-Garhy HAS (2021). Exogenously Applied Chitosan and Chitosan Nanoparticles Improved Apple Fruit Resistance to Blue Mold, Upregulated Defense-Related Genes Expression, and Maintained Fruit Quality. Horticulturae 7(8):224.

El-Aziz AR, Al-Othman MR, Mahmoud MA, Shehata SM, Abdelazim NS (2018). Chitosan Nanoparticles as a Carrier for *Mentha longifolia* Extract: Synthesis, Characterization and Antifungal Activity. Current Science 114(10):2116-2122.

Amighi M, Zahedifar M, Alizadeh H, Payandeh M (2023). Encapsulation of Nepeta hormozganica and Nepeta dschuprensis essential oils in shrimp chitosan NPs: Enhanced antifungal activity. International Journal of Biological Macromolecules 238:124112.

Anitha A, Deepagan VG, Divya Rani VV, Menon D, Nair SV, Jayakumar R (2011). Preparation, characterization, in vitro drug release and biological studies of curcumin loaded dextran sulphate–chitosan nanoparticles. Carbohydrate Polymers 84(3):1158-1164.

Ayesha MS, Suryanarayanan TS, Nataraja KN, Prasad SR, Shaanker RU (2021). Seed Treatment with Systemic Fungicides: Time for Review. Frontiers in Plant Science 12:654512. https://doi.org/10.3389/fpls.2021.654512

Bagheri R, Ariaii P, Motamedzadegan A (2021). Characterization, antioxidant and antibacterial activities of chitosan nanoparticles loaded with nettle essential oil. Journal of Food Measurement and Characterization 15(2):1395-1402.

Bassolé IHN, Juliani HR (2012). Essential Oils in Combination and Their Antimicrobial Properties. Molecules 17(4):3989-4006.

Beatrice C, Linthorst JMH, Cinzia F, Luca R (2017). Enhancement of PR1 and PR5 gene expressions by chitosan treatment in kiwifruit plants inoculated with *Pseudomonas syringae* pv. *actinidiae*. European Journal of Plant Pathology 148(1):163-179.

Begines B, Ortiz T, Pérez-Aranda M, Martínez G, Merinero M, Argüelles-Arias F, Alcudia A (2020). Polymeric Nanoparticles for Drug Delivery: Recent Developments and Future Prospects. Nanomaterials 10(7):1403.

Bouissil S, Guérin C, Roche J, Dubessay P, Alaoui-Talibi ZE, Pierre G, Michaud P, Mouzeyar S, Delattre C, Modafar CE (2022). Induction of Defense Gene Expression and the Resistance of Date Palm to *Fusarium oxysporum* f. sp. Albedinis in Response to Alginate Extracted from Bifurcaria bifurcata. Marine Drugs 20(2):88. https://doi.org/10.3390/md20020088

Cai J, Yang D, Wang Q (2023). Preparation and characterization of chitosan nanoparticles loaded with Athyrium sinense essential oil with antibacterial properties against *Pectobacterium carotovorum* subsp. carotovorum. Industrial Crops and Products 195:116382. https://doi.org/10.1016/j.indcrop.2023.116382

Chun SC, Chandrasekaran M (2019). Chitosan and chitosan nanoparticles induced expression of pathogenesis-related proteins genes enhances biotic stress tolerance in tomato. International Journal of Biological Macromolecules 125:948-954.

Devi NO, Devi R, Debbarma M, Hajong M, Thokchom S (2022). Effect of endophytic Bacillus and arbuscular mycorrhiza fungi (AMF) against Fusarium wilt of tomato caused by *Fusarium oxysporum* f. sp. lycopersici. Egyptian Journal of Biological Pest Control 32:1-14.

Dey P, Ramanujam R, Venkatesan G, Radhakrishnan N (2019). Sodium alginate potentiates antioxidant defense and PR proteins against early blight disease caused by Alternaria solani in *Solanum lycopersicum* Linn. PLoS One 14(9):e0223216.

Hadidi M, Pouramin S, Adinepour F, Haghani S, Jafari SM (2020). Chitosan nanoparticles loaded with clove essential oil: Characterization, antioxidant and antibacterial activities. Carbohydrate Polymers 236:116075.

Haider J, Majeed H, Williams PA, Safdar W, Zhong F (2017). Formation of chitosan nanoparticles to encapsulate krill oil (*Euphausia superba*) for application as a dietary supplement. Food Hydrocolloids 63:27-34.

Hoang NH, Le Thanh T, Sangpueak R, Treekoon J, Saengchan C, Thepbandit W, Papathoti NK, Kamkaew A, Buensanteai N (2022). Chitosan Nanoparticles-Based Ionic Gelation Method: A Promising Candidate for Plant Disease Management. Polymers 14(4):662. https://doi.org/10.3390/polym14040662

Hosseini SF, Zandi M, Rezaei M, Farahmandghavi F (2013). Two-step method for encapsulation of oregano essential oil in chitosan nanoparticles: Preparation, characterization and in vitro release study. Carbohydrate Polymers 95(1):50-56.

Jia L, Wang R, Fan Y (2020). Encapsulation and release of drug nanoparticles in functional polymeric vesicles. Soft Matter 16(12):3088-3095.

Jian W, Khelissa S, Chihib N, Dumas É, Gharsallaoui A. (2019). Effect of drying and interfacial membrane composition on the antimicrobial activity of emulsified citral. Food Chemistry 298:125079. https://doi.org/10.1016/j.foodchem.2019.125079

Kalagatur NK, Nirmal Ghosh OS, Sundararaj N, Mudili V (2018). Antifungal Activity of Chitosan Nanoparticles Encapsulated with *Cymbopogon martinii* Essential Oil on Plant Pathogenic Fungi *Fusarium graminearum*. Frontiers in Pharmacology 9:610. https://doi.org/10.3389/fphar.2018.00610

Kalleli F, Abid G, Salem IB, Boughalleb-M'Hamdi N, Mahmoud MA (2020). Essential oil from fennel seeds (Foeniculum vulgare) reduces Fusarium wilt of tomato (*Solanum lycopersicon*). (DOAJ: Directory of Open Access Journals). https://doi.org/10.14601/phyto-11143

Kaur G, Ganjewala D, Bist V, Verma PC (2019). Antifungal and larvicidal activities of two acyclic monoterpenes; citral and geraniol

against phytopathogenic fungi and insects. Archives of Phytopathology and Plant Protection 52(5-6):458-469.
Keawchaoon L, Yoksan R (2011). Preparation, characterization and in vitro release study of carvacrol-loaded chitosan nanoparticles. Colloids and surfaces B: Biointerfaces 84(1):163-171.
Khanmohammadi M, Elmizadeh H, Ghasemi K (2015). Investigation of size and morphology of chitosan nanoparticles used in drug delivery system employing chemometric technique. PubMed 14(3):665-675.
Kiirika LM, Stahl F, Wydra K (2013). Phenotypic and molecular characterization of resistance induction by single and combined application of chitosan and silicon in tomato against *Ralstonia solanacearum*. Physiological and Molecular Plant Pathology 81:1-12.
La Torre A, Caradonia F, Matere A, Battaglia V (2016). Using plant essential oils to control Fusarium wilt in tomato plants. European Journal of Plant Pathology 144(3):487-496.
Lammari N, Louaer O, Meniai AH, Elaissari A (2020). Encapsulation of Essential Oils via Nanoprecipitation Process: Overview, Progress, Challenges and Prospects. Pharmaceutics 12(5):431.
Li J, Zhou X, Zhang C, Zhao Y, Zhu Y, Zhang J, Bai J, Xiao X (2020). The Effects of Carbendazim on Acute Toxicity, Development, and Reproduction in *Caenorhabditis elegans*. Journal of Food Quality 2020:1-6.
Linde JH, Combrinck S, Regnier TJC, Virijevic S (2010). Chemical composition and antifungal activity of the essential oils of *Lippia rehmannii* from South Africa. South African Journal of Botany 76(1):37-42.
Liu G, An D, Li J, Deng S (2023). Zein-based nanoparticles: Preparation, characterization, and pharmaceutical application. Frontiers in Pharmacology 14:1120251.
Lü W, Huang DW, Wang CC, Yeh C, Tsai JC, Huang Y, Li PH (2018). Preparation, characterization, and antimicrobial activity of nanoemulsions incorporating citral essential oil. Journal of Food and Drug Analysis 26(1):82-89.
Ma H, Zhao Y, Lu Z, Xing R, Yao X, Jin Z, Wang Y, Yu F (2020). Citral-loaded chitosan/carboxymethyl cellulose copolymer hydrogel microspheres with improved antimicrobial effects for plant protection. International Journal of Biological Macromolecules 164:986-993.
Marei GIK, Rabea EI, Badawy ME (2018). Preparation and Characterizations of Chitosan/Citral Nanoemulsions and their Antimicrobial Activity. (DOAJ: Directory of Open Access Journals). https://doi.org/10.22037/afb.v5i2.19005
Maswal M, Dar AA (2014). Formulation challenges in encapsulation and delivery of citral for improved food quality. Food Hydrocolloids 37:182-195.
Nagpal K, Singh SK, Mishra DN (2010). Chitosan nanoparticles: a promising system in novel drug delivery. Chemical and Pharmaceutical Bulletin 58(11):1423-1430.
Nunes MR, Agostinetto L, Da Rosa CG, Sganzerla WG, Pires MF, Munaretto GA, Rosar CR, Bertoldi FC, Barreto PLM, De Lima Veeck AP, Zinger FD (2024). Application of nanoparticles entrapped orange essential oil to inhibit the incidence of phytopathogenic fungi during storage of agroecological maize seeds. Food Research International 175:113738. https://doi.org/10.1016/j.foodres.2023.113738
Oleandro E, Stanzione M, Buonocore GG, Lavorgna M (2024). Zein-Based nanoparticles as active platforms for Sustainable applications: recent advances and perspectives. Nanomaterials 14(5):414. https://doi.org/10.3390/nano14050414
Oluoch G, Matiru V, Mamati EG, Nyongesa M (2021). Nanoencapsulation of Thymol and Eugenol with Chitosan Nanoparticles and the Effect against *Ralstonia solanacearum*. Advances in Microbiology 11(12):723-739.
Rasteh I, Pirnia M, Miri MA, Sarani S (2024). Encapsulation of *Zataria multiflora* essential oil in electrosprayed zein microcapsules: Characterization and antimicrobial properties. Industrial Crops and Products 208:117794. https://doi.org/10.1016/j.indcrop.2023.117794
Santos CMD, De Araújo Gonçalves M, De Macedo LF, Torres AHF, Marena GD, Chorilli M, Trovatti E (2023). Green nanotechnology for the development of nanoparticles based on alginate associated with essential and vegetable oils for application in fruits and seeds protection. International Journal of Biological Macromolecules 232:123351. https://doi.org/10.1016/j.ijbiomac.2023.123351
Scorzoni L, Sangalli-Leite F, De Lacorte Singulani J, De Paula E Silva ACA, Costa-Orlandi CB, Fusco-Almeida AM, Mendes-Giannini MJS (2016). Searching new antifungals: The use of *in vitro* and *in vivo* methods for evaluation of natural compounds. Journal of Microbiological Methods 123:68-78.
Servat-Medina L, González-Gómez A, Reyes-Ortega F, Sousa IMO, Queiroz NDCA, Zago PMW, Jorge MP, Monteiro KM, Carvalho JE, San Román J, Foglio MA (2015). Chitosan tripolyphosphate nanoparticles as *Arrabidaea chica* standardized extract carrier: Synthesis, characterization, biocompatibility, and antiulcerogenic activity. International Journal of Nanomedicine pp. 3897-3909.
Sharma A, Harjai K, Ramniwas S, Singh D (2023). Bioactivity of Citral and Its Nanoparticle in Attenuating Pathogenicity of *Pseudomonas aeruginosa* and Controlling *Drosophila melanogaster*. Journal of Nanomaterials 2023:1-11.
Sharma A, Rajendran S, Srivastava A, Sharma S, Kundu B (2017). Antifungal activities of selected essential oils against *Fusarium oxysporum* f. Sp. *lycopersici* 1322, with emphasis on *Syzygium aromaticum* essential oil. Journal of Bioscience and Bioengineering 123(3):308-313.
Shetta A, Kegere J, Mamdouh W (2019). Comparative study of encapsulated peppermint and green tea essential oils in chitosan nanoparticles: Encapsulation, thermal stability, in-vitro release, antioxidant and antibacterial activities. International Journal of Biological Macromolecules 126:731-742.
Srinivas C, Devi D, Murthy KN, Mohan CD, Lakshmeesha TR, Singh BP, Kalagatur NK, Niranjana SR, Hashem A, Tabassum B, Nayaka SC (2019). *Fusarium oxysporum* f. sp. *lycopersici* causal agent of vascular wilt disease of tomato: Biology to diversity– A review. Saudi Journal of Biological Sciences 26(7):1315-1324.
Tian H, Lu Z, Li D, Hu J (2018). Preparation and characterization of citral-loaded solid lipid nanoparticles. Food Chemistry 248:78-85.
Wei L, Chen C, Chen J, Lin L, Wan C (2021). Possible fungicidal effect of citral on kiwifruit pathogens and their mechanisms of actions. Physiological and Molecular Plant Pathology 114:101631. https://doi.org/10.1016/j.pmpp.2021.101631
Worrall E, Hamid A, Mody K, Mitter N, Pappu H (2018). Nanotechnology for Plant Disease Management. Agronomy 8(12):285. https://doi.org/10.3390/agronomy8120285
Xing K, Zhu X, Peng X, Qin S (2015). Chitosan antimicrobial and eliciting properties for pest control in agriculture: A review. Agronomy for Sustainable Development 35(2):569-588.
Yammine J, Chihib N, Gharsallaoui A, Ismail A, Karam L (2023). Advances in essential oils encapsulation: development, characterization and release mechanisms. Polymer Bulletin 81(5):3837-3882.
Yang L, Wen KS, Ruan X, Zhao YX, Wei F, Wang Q (2018). Response of Plant Secondary Metabolites to Environmental Factors. Molecules 23(4):762. https://doi.org/10.3390/molecules23040762
Yassin MT, Mostafa AAF, Al-Askar AA (2021). *In vitro* antagonistic activity of *Trichoderma harzianum* and *T. viride* strains compared to carbendazim fungicide against the fungal phytopathogens of *Sorghum bicolor* (L.) Moench. Egyptian Journal of Biological Pest Control 31(1):118. https://doi.org/10.1186/s41938-021-00463-w
Zhao X, Zhang Y, Chen L, Ma Z, Zhang B (2023). Chitosan-thymol nanoparticle with pH responsiveness as a potential intelligent botanical fungicide against *Botrytis cinerea*. Pesticide Biochemistry and Physiology 195:105571. https://doi.org/10.1016/j.pestbp.2023.105571
Zhu G, Feng N, Xiao Z, Zhou R, Niu Y (2015). Production and pyrolysis characteristics of citral–monochlorotriazinyl-β-cyclodextrin inclusion complex. Journal of Thermal Analysis and Calorimetry 120(3):1811-1817.